This document is the accepted manuscript version of the following article:
Schilling, I. E., Bopp, C. E., Lal, R., Kohler, H. P. E., & Hofstetter, T. B. (2019). Assessing aerobic biotransformation of hexachlorocyclohexane isomers by compound-specific isotope analysis. Environmental Science and Technology, 53(13), 7419-7431. https://doi.org/10.1021/acs.est.9b01007

Assessing Aerobic Biotransformation of Hexachlorocyclohexane Isomers by Compound-Specific Isotope Analysis

Iris E. Schilling,[†,‡] Charlotte E. Bopp,[†,‡] Rup Lal,[¶] Hans-Peter E. Kohler,[*,†,‡] and Thomas B. Hofstetter[*,†,‡]

Eawag, Swiss Federal Institute of Aquatic Science and Technology, CH-8600 Dübendorf, Switzerland, Institute of Biogeochemistry and Pollutant Dynamics, ETH Zürich, CH-8092 Zürich, Switzerland, and Department of Zoology, University of Delhi, Delhi 110007, India

E-mail: hanspeter.kohler@eawag.ch; thomas.hofstetter@eawag.ch

[*]To whom correspondence should be addressed
[†]Eawag
[‡]ETH Zürich
[¶]University of Delhi

Abstract

Contamination of soils and sediments with the highly persistent hexachlorocyclohexanes (HCHs) continues to be a threat for humans and the environment. Despite the existence of bacteria capable of biodegradation and cometabolic transformation of HCH isomers, such processes occur over timescales of decades and are thus challenging to assess. Here, we explored the use of compound-specific isotope analysis to track the aerobic biodegradation and biotransformation pathways of the most prominent isomers, namely (−)-α-, (+)-α-, β-, γ-, and δ-HCH through changes of their C and H isotope composition in assays of LinA2 and LinB enzymes. Dehydrochlorination of (+)-α-, γ-, and δ-HCH catalyzed by LinA2 was subject to substantial C and H isotope fraction with apparent ^{13}C- and ^{2}H-kinetic isotope effects (AKIEs) of up to 1.029 ± 0.001 and 6.7 ± 2.9, respectively, which are indicative of bimolecular eliminations. Hydrolytic dechlorination of δ-HCH by LinB exhibited even larger C but substantially smaller H isotope fractionation with ^{13}C- and ^{2}H-AKIEs of 1.073 ± 0.006 and 1.41 ± 0.04, respectively, that are typical for nucleophilic substitutions. The systematic evaluation of isomer-specific phenomena showed that in addition to contaminant uptake limitations, diffusion-limited turnover ((−)-α-HCH), substrate dissolution (β-HCH), and potentially competing reactions catalyzed by constitutively expressed enzymes might bias the assessment of HCH biodegradation by CSIA at contaminated sites.

Introduction

Hexachlorocyclohexane (HCH) was one of the first commercial and one of the most extensively used organochlorine pesticides.[1,2] From the 1940s to the 1990s, HCH was intensively used in agriculture, forestry, and public health.[2,3] Technical HCH was produced by photochlorination of benzene yielding a mixture of the stable isomers α-HCH (60 to 70%), β-HCH (5 to 12%), γ-HCH (8 to 15%), δ-HCH (6 to 10%), and ϵ-HCH (3 to 4%).[1,4,5] Application of technical HCH was common until the 1950ies, even though it was known that only the γ-HCH isomer had insecticidal properties.[6] Starting in 1953, technical HCH was replaced by the pure γ-isomer, which was marketed under the brand name "Lindane". γ-HCH was produced by fractional crystallization, a process in which 85% to 92% of the material was left as isomeric waste that was often dumped in the environment.[1,7]

Although HCHs have been banned for use as pesticides and have been added to the list of persistent organic pollutants (POP) under the Stockholm convention,[1,2] HCH residues still occur in various environmental compartments in concentrations of up to several g kg^{-1} posing serious environmental problems.[2,8–10] Especially for clean-up of farmland that is polluted by HCH at relatively low concentrations (μg kg^{-1}), bioremediation through aerobic HCH biodegradation has been suggested to be a viable option for clean up.[8,11–14] An important prerequisite for successful bioremediation, however, is a thorough understanding of the extent and the nature of transformation processes at contaminated sites. Monitoring such processes through changes of contaminant stable isotope ratios by compound-specific isotope analysis (CSIA) is well suited for site assessments. Applications of CSIA to HCH isomers,[15–23] however, are currently limited because of the complex biochemistry of isomer-specific degradation and transformation pathways observed under aerobic conditions.[7,15,24–29] Biochemical complexity arises because, firstly, mineralization by HCH-transforming strains could only be established unequivocally for γ-HCH. Secondly, the other isomers (α-, β-, δ-, and ϵ-HCH) are mainly cometabolically transformed to dehydrochlorinated and hydroxylated metabolites by lindane dehydrochlorinase (LinA) and haloalkane dehalogenase (LinB), respectively, the first two enzymes of the γ-HCH degradation pathway. Thirdly, in many

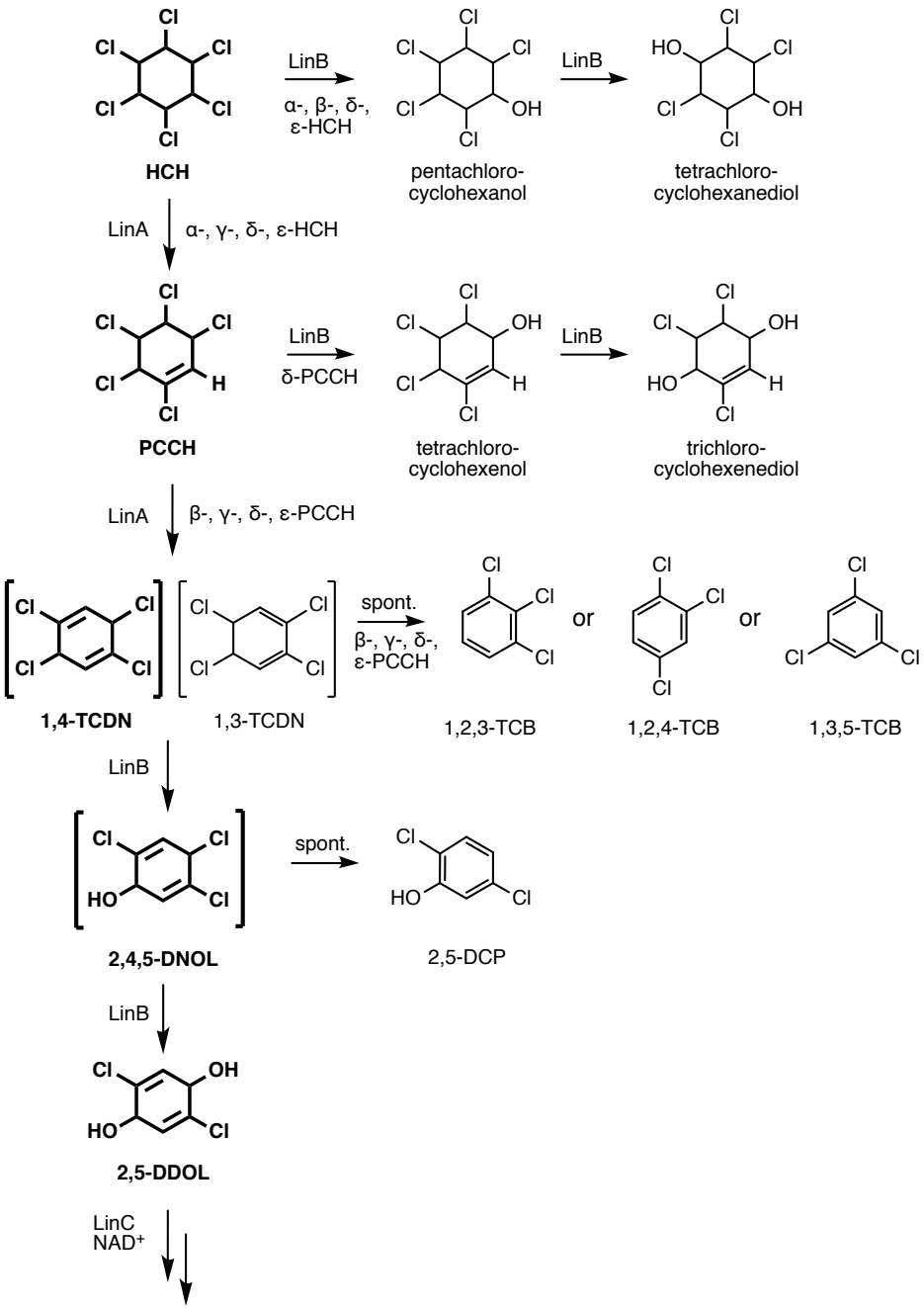

Scheme 1 Generalized reaction network for the transformation of HCH (hexachlorocyclohexane) isomers under aerobic conditions. The main vertical reaction pathway of γ-HCH is highlighted in bold. Deviations from this pathway are shown horizontally to the main pathway. Trichlorobenzenes (TCB) and 2,5-dichlorophenol (2,5-DCP) are assumed to be formed by spontaneous elimination reactions (spont.). When incubated with LinB, HCHs and some PCCHs (pentachlorocyclohexenes) are hydrolytically dechlorinated to pentachlorocyclohexanols and further to tetrachlorocyclohexanediols. Other abbrevations used: TCDN for tetrachlorocyclohexadiene, 2,4,5-DNOL for 2,4,5-trichloro-2,5-cyclohexadiene-1-ol, and 2,5-DDOL for 2,5-dichloro-2,5-cyclohexadiene-1,4-diol.[8] For more detailed chemical structures see Figures S4 and S5.

instances LinA and LinB compete for the same substrates.[8,11,24] Scheme 1 comprises the most relevant dehydrochlorination and hydrolytic dechlorination reactions catalyzed by LinA and LinB, respectively, and in Figures S4 and S5, we present the chemical structures of the corresponding HCH isomers and metabolites. The productive pathway enabling growth on γ-HCH is shown in bold as vertical reaction pathway initiated by sequential reactions of LinA. LinB, which is responsible for hydroxylation of tetra- and trichlorinated intermediates derived from γ-HCH, also competes with LinA for several HCH and pentachlorocyclohexene (PCCH) isomers at other stages in the reaction network.

The goal of this work was to address the consequences of the biochemical complexity of the HCH transformation network for applications of CSIA. While CSIA at contaminated environments comprise the evaluation of the most important HCH isomers (i.e, (−)-α-, (+)-α-, β-, γ-, and δ-HCH),[17,18,21] experimental data on isotope fractionation trends associated with aerobic biodegradation is scarce and limited to a laboratory study with α- and γ-HCH isomers[20] (see compilation in Section S5.2). The current work focuses on a comprehensive investigation of isomer-specific effects on the isotope fractionation associated with aerobic HCH biodegradation, namely on enzyme-catalyzed dehydrochlorination and hydrolytic dechlorination reactions. To that end, we systematically present results on the magnitude and variability of C and H isotope fractionation of LinA- and LinB-catalyzed reactions with (−)-α-, (+)-α-, β-, γ-, and δ-HCH as well as on the transformation kinetics of these HCH isomers to less chlorinated products in enzyme assays containing LinA2 or LinB. This work also includes data on the dehydrochlorination of γ-HCH from our previous study,[15] in which we addressed the effect of conformational mobility of HCHs and where we established the experimental, analytical, and data evaluation procedures required for the current study. Based on the apparent ^{13}C- and ^{2}H-kinetic isotope effects (AKIEs) and the catalytic efficiencies of LinA2 and LinB for five different HCH isomers, we discuss substrate- and enantiomer-specific differences in the dehydrochlorination and hydrolytic dechlorination mechanisms. The insights from our work in laboratory model systems have important implications for a successful application of CSIA at contaminated sites by illustrating that, in addition to

contaminant uptake limitations, diffusion-limited turnover, substrate dissolution, and potentially competing reactions catalyzed by constitutively expressed enzymes might bias the assessment of HCH biodegradation.

Materials and Methods

Chemicals and Protein Purification Procedures

In the Supporting Information Section S1, a complete list of chemicals, their suppliers and purities can be found. Chemical structures of substrates, products, tentative reaction intermediates, and stereoisomers of PCCH are shown in Figures S4 and S5. Procedures for the purification of LinA2 and LinB from *Sphingobium indicum* B90A that were expressed in *E. coli* BL21AI are provided in Section S2. Growth procedures, induction of enzyme expression, and enzyme purification for LinA2 were established previously,[15] and LinB was produced accordingly.

Biotransformation Experiments

We performed the transformation experiments for each enzyme-HCH-isomer combination separately. As shown in Section S3 and Table S1, 0.8 to 35 μM of HCH was incubated with 0.003 to 14.5 μg mL^{-1} of purified enzyme in 150 to 800 mL tris-glycine buffer at pH 7.5 (200 mM glycine, 25 mM Trizma® base) and 0.1 to 1 vol-% of acetone depending on the solubility of the HCH isomer. Experiments were carried out at room temperature on an orbital shaker at 100 rpm (KS15A or SM 30A, Edmund Bühler GmbH). A total of 10 to 14 reactors, sealed with viton rubber stoppers (Maagtechnic AG), were set up for each experiment. At predefined time-points, reactors were sacrificed by stopping the reaction through extraction of the analytes into *n*-hexane or ethyl acetate for at least 2 min. All substrates and products listed in Figure S4 were extracted into the *n*-hexane before opening the reactors (Table S1). Exceptions include pentachlorocyclohexanol (labelled B1 according to nomenclature proposed by Geueke et al.[24] as shown in Figure S4) and

tetrachlorocyclohexanediol (B2) from β-HCH which were extracted into ethyl acetate (Table S1). *n*-Hexane and ethyl acetate contained 20 μM of 2,4-dinitrotoluene as internal standard, to account for solvent evaporation during sample preparation.

Chemical and Isotopic Analyses

The concentrations of substrates and products were analyzed using a Trace GC Ultra with ITQ 900 (Thermo Scientific) gas chromatography/mass spectrometry device (GC/MS). GC-columns and temperature programs applied in experiments with different HCH isomers are listed in Table S1. The amounts of substrate and product were determined from peak areas relative to those of external standard curves. The concentrations of PCCHs, pentachlorocyclohexanols, and tetrachlorocyclohexanediols, for which no standards were available, were approximated with response factors determined at m/z values of representative ions. The response factor for PCCH isomers was obtained at m/z 181 during the initial stages of HCH transformation when the amount of HCH transformed by LinA2 would correspond to the amount of PCCH formed.[15] The identical procedure was applied to obtain a response factor for pentachlorocyclohexanols at m/z of 199 from the reaction of HCH isomers with LinB based on mass spectra published previously.[25,30] The concentration of tetrachlorocyclohexanediols was obtained after substracting the concentrations of HCH and PCCH from the initial HCH concentration.

$^{13}C/^{12}C$ ratios of α-, β-, and δ-HCH, as well as PCCHs, pentachlorocyclohexanols, and tetrachlorocyclohexanediols and $^{2}H/^{1}H$ ratios of α-, β-, and δ-HCH were determined by gas chromatography/isotope ratio mass spectrometry (GC/IRMS, Trace GC, Delta plus XL/Delta V plus equipped with GC combustion III interface, all Thermo Scientific) as described in Schilling et al.[15] Details on GC-columns and temperature programs for concentration and isotope analysis of the analytes are listed in Table S1 according to the substrate used in each experiment. Note that the low chromatographic resolution of $^{2}H/^{1}H$ ratio measurements precluded baseline separation of α-HCH enantiomers.

HCH-containing solvent extracts were analyzed for $^{13}C/^{12}C$ and $^{2}H/^{1}H$ ratios using standard

bracketing procedures.[31] C and H isotope signatures, $\delta^{13}C$ and $\delta^{2}H$, are reported as arithmetic means of three- and fivefold measurements relative to Vienna PeeDee Belemnite ($\delta^{13}C_{VPDB}$) or Vienna Standard Mean Ocean Water ($\delta^{2}H_{VSMOV}$), respectively. Isotopic calibration and measurement uncertainties of multiple injections were accounted for by using a Kragten spreadsheet[32] as proposed by Dunn et al.[33]

Data Analysis

Reaction kinetics

The transformation kinetics of HCH isomers to less chlorinated products were evaluated in a series of ordinary differential equations solved in Copasi.[34] In cases of enzyme inhibition, the initial concentrations were adjusted for the amount of residual substrate prior to evaluation of reaction kinetics. The catalytic efficiencies, k_{cat}/K_m (in M^{-1} s^{-1}), of the reactions catalyzed by LinA2 and LinB were determined under the assumption of Michaelis-Menten kinetics as shown previously.[15] Due to the limited aqueous solubility of HCH isomers (<50 μM),[35,36] experiments were conducted at aqueous substrate concentrations below enzyme saturation, that is at $S \ll K_m$. These boundary conditions preclude separate quantification of k_{cat} and K_m, and the Michaelis-Menten expression then modifies to eq 1.

$$v = \frac{k_{cat}}{K_m} \cdot [Enz]_0 \cdot [S] = k_{obs,S} \cdot [S] \quad (1)$$

$$\frac{k_{cat}}{K_m} = \frac{k_{obs,S}}{[Enz]_0} \quad (2)$$

where v is the reaction rate in M s^{-1}, k_{cat} the turnover number in s^{-1}, K_m is the Michaelis constant in M, $[Enz]_0$ is the initial enzyme concentration in M, $[S]$ is the substrate concentration in M, and $k_{obs,S}$ is the first order reaction rate constant of substrate disappearance in s^{-1}. $[Enz]_0$ was calculated from the molar mass of the amino acid sequences (17 341 g mol^{-1} for LinA2 and 33 108 g mol^{-1} for LinB).[37] k_{cat}/K_m-values were obtained from eq 2.

Stable Isotope Analyses

Bulk C and H isotope enrichment factors, ϵ_C and ϵ_H, of element E were obtained from non-linear regression of eq 3 using Igor Pro (WaveMetrics) as described in Section S4.2.

$$\frac{\delta^h E + 1}{\delta^h E_0 + 1} = \left(\frac{c}{c_0}\right)^{\epsilon_E} \tag{3}$$

where E stands for the isotopic element (C or H), $\delta^h E_0$ is the initial isotope signature of element E, $\delta^h E$ is the isotope signature of E at any time-point during the reaction, and c/c_0 is the fraction of remaining substrate. Data from multiple data sets were combined through procedures described in Scott et al.[38] ϵ_E-values were also approximated from the difference of substrate and dechlorinated product isotope signatures at low substrate turnover ($c/c_0 \geq 0.9$, eq 4).[31]

$$\epsilon_E \approx \delta^h E_{product} - \delta^h E_{substrate_{t=0}} \tag{4}$$

Apparent ^{13}C-kinetic isotope effects for the transformation of HCH isomers by LinA2 and LinB were determined with eq 5.

$$^{13}C\text{-AKIE} = \frac{1}{1 + n/x \cdot z \cdot \epsilon_C} \tag{5}$$

where n is the number of C atoms, x is the number of such atoms at reactive positions, and z is the correction for intramolecular isotopic competition[39] as summarized in Table S3. An analogous form of eq 5 was used for determining ^2H-AKIEs for hydrolytic dechlorinations of HCH isomers catalyzed by LinB with the corresponding parameter values for H atoms (Table S3). To derive ^2H-AKIEs for HCH dehydrochlorination by LinA2, we solved a set of ordinary differential equations,[31,40] that included HCH isotopomers containing either only ^1H or one ^2H atom as shown recently in Schilling et al.[15]. Input parameters are listed and discussed in Section S4.2. Differential equations were solved in Aquasim[41] by fitting measured species concentrations and H isotope ratios to eq S7 and the ^2H-AKIE was then obtained from eq 6.

$$^{2}\text{H-AKIE} = \frac{^{2\text{H}}k}{^{1\text{H}}k} \tag{6}$$

where $^{1\text{H}}k$ and $^{2\text{H}}k$ are the rate constants for the reaction of light and heavy H isotopologues of the substrate, respectively (eq S7). Due to the large H isotope effects associated with the dehydrochlorination of HCHs by LinA2,[15] the correlation of C and H isotope fractionation, $\Lambda^{\text{H/C}}$, was evaluated with eq 7.[40,42]

$$\Lambda^{\text{H/C}} = \frac{\ln\left(\left(\delta^{2}\text{H} + 1\right)/\left(\delta^{2}\text{H}_0 + 1\right)\right)}{\ln\left(\left(\delta^{13}\text{C} + 1\right)/\left(\delta^{13}\text{C}_0 + 1\right)\right)} = \frac{\epsilon_{\text{H}}}{\epsilon_{\text{C}}} \tag{7}$$

where $\Lambda^{\text{H/C}}$ was the slope of the linear regression of δ^{2}H *vs.* δ^{13}C which corresponds to the ratio of isotope enrichment factors, $\epsilon_{\text{H}}/\epsilon_{\text{C}}$.

Due to the lack of chromatographic resolution for $^{2}\text{H}/^{1}\text{H}$ ratio measurements of α-HCH enantiomers, H isotope fractionation could only be evaluated quantitatively for the less reactive enantiomer (+)-α-HCH once the more reactive enantiomer (−)-α-HCH had disappeared. The ϵ_{H}-values derived from this data depended on assumptions for the initial δ^{2}H-values of (+)-α and (−)-α-HCHs as documented in model calculations shown in Section S4.3.

Results

LinA2-catalyzed transformation reactions

Incubation of LinA2 with α- and δ-HCH led to their transformation by dehydrochlorination. β-HCH was not transformed by LinA2 (Figure S7) consistent with previous findings that β-HCH is not a substrate of LinA.[8] Catalytic efficiencies, $k_{\text{cat}}/K_{\text{m}}$, isotope enrichment factors, ϵ, and apparent kinetic isotope effects, AKIE, for dehydrochlorination of α- and δ-HCH are compiled in Table 1 together with data for γ-HCH obtained recently.[15]

δ-HCH

δ-HCH was completely transformed within 9 hours when incubated with LinA2 (Figure 1A). δ-PCCH was observed as an intermediate that transformed to 1,2,3- and 1,2,4-TCB. At the end of the incubations, the sum of substrate and metabolite concentrations matched the initial substrate concentration, which indicated a complete mass balance. The changes of δ^{13}C values of δ-HCH and of its products are shown in Figure 1B. The C isotope enrichment factor, ϵ_C, for the dehydrochlorination of δ-HCH was -9.1 ± 0.4 ‰ (eq 3). δ^{13}C values of δ-PCCH showed the typical isotope enrichment of a transient product. Initially, δ-PCCH was depleted in ^{13}C, and in the course of the reaction, it became enriched in ^{13}C. As accumulating final product, 1,2,4-TCB was depleted in ^{13}C relative to δ-HCH and δ-PCCH but only accounted for approx. 15% of the transformed substrate. Figure 1C shows the strong H isotope fractionation of δ-HCH for the LinA2-catalyzed transformation reaction. The H isotope enrichment factor, ϵ_H, amounted to 182 ± 18‰ (Table 1).

α-HCH

When incubating racemic α-HCH with LinA2, the (–)-enantiomer, (−)-α-HCH, was transformed much faster than the (+)-enantiomer, (+)-α-HCH (Table 1, Figures 1D and G), consistent with previous work.[27,43] To analyze the reaction progress of both enantiomers in an optimal range, we set up two separate incubations. Data for (−)-α-HCH were obtained when racemic α-HCH was incubated with LinA2 at a low enzyme concentration (0.01 μg mL^{-1}), whereas data for (+)-α-HCH were obtained with incubations at a high enzyme concentration (0.7 μg mL^{-1}).

Out of four theoretically possible PCCH stereoisomers generated through dehydrochlorination of (−)-α- and (+)-α-HCH, (Figure S6), only the two β-PCCH enantiomers were formed in these incubations. (−)-α-HCH was exclusively transformed to β-PCCH**2** and (+)-α-HCH exclusively to β-PCCH**1** (Figures 1D, G and S6). Subsequently, both β-PCCH enantiomers were further transformed to 1,2,4-TCB, except in the incubations at low enzyme concentrations, in which the reaction ceased after 20 min without formation of 1,2,4-TCB. At the end of the experiments, the

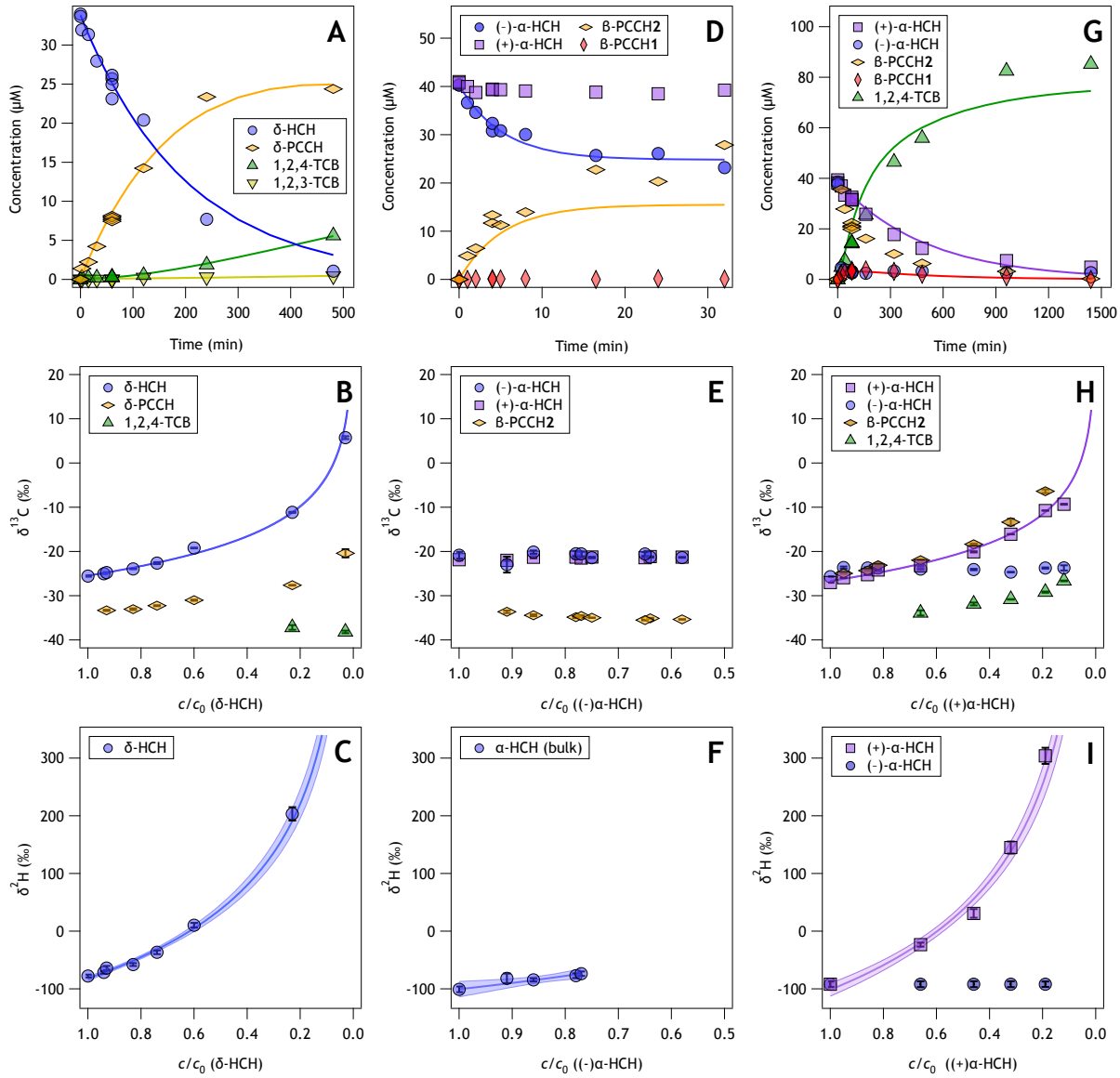

Figure 1 Concentration trends and C and H isotope fractionation associated with the dehydrochlorination of δ-HCH (panels A-C) and α-HCH (panels D-I) in assays with LinA2 at pH 7.5. Panels D to F and G to I show the results of two separate experiments with 0.01 and 0.7 μg LinA2 mL^{-1}, respectively. The top row, panels A, D, and G, shows measured and approximated concentrations of substrates and all products and the solid lines represent best fits obtained for solving a series of ordinary differential equations.[34] The second row, panels B, E, and H, illustrates C isotope fractionation of substrate and products. The third row, panels C, F, and I, reports H isotope fractionation of the substrates. Solid lines in isotope fractionation plots (B-C, E-F, H-I) represent non-linear fits to eq 3 and the shaded ares are 95% confidence intervals. Note that x-axes in panels E and F only show the first 50% of substrate disappearance, i.e., $c/c_0 > 0.5$ and that δ^{13}C values for $(+)$-α-HCH in panel E are plotted vs. c/c_0 of $(-)$-α-HCH.

concentration of unreacted substrates and that of metabolites formed matched the initial substrate concentration.

(−)-α-HCH In experiments at low enzyme concentration (0.01 μg mL^{-1}), (−)-α-HCH transformation stopped after about 20 min (Figure 1D) when only approx. 35% had disappeared. The expected final transformation product, 1,2,4-TCB[27] could not be detected. In experiments at high enzyme concentration (0.7 μg mL^{-1}), the concentration of (−)-α-HCH decreased rapidly within 20 min and then remained constant at about 3 μM until the end of the experiment (Figure 1G).

Contrary to observations with other HCH isomers, there was no change in the δ^{13}C of (−)-α-HCH throughout its reaction in experiments with high and low enzyme concentrations. We also did not measure any change in δ^{13}C of the reaction product β-PCCH**2** throughout the reaction at low enzyme concentration (Figure 1E; note that the x-axis only scales to 50% reactant conversion). However, β-PCCH**2** was depleted in ^{13}C and the δ^{13}C values of (−)-α-HCH and β-PCCH**2** differed by -11.7 ± 1.5‰. This difference corresponds to a C isotope enrichment factor, ϵ_C, of the same magnitude (eq 4). In contrast, in the experiment at high enzyme concentration, the C isotope signatures of (−)-α-HCH (-25.7 ± 0.1‰) and β-PCCH**2** (-25.0 ± 0.1‰) differed only by -0.7 ± 0.1‰ early in the reaction (i.e., $c/c_0 \geq 0.9$, Figure 1H). However, it needs to be noted that we could not separate the two β-PCCH enantiomers for C isotope ratio measurements. Since β-PCCH**1** was only present at minimal concentrations, especially after 20 min, we attributed the measured signature solely to β-PCCH**2**. We also observed H isotope fractionation of α-HCH during the dehydrochlorination reaction (Figure 1F) corresponding to an ϵ_H of -113 ± 78‰. Due to the lack of chromatographic resolution of α-HCH enantiomers during ^{2}H/^{1}H-ratio analysis and the concomitant reaction of a small amount of (+)-α-HCH, this ϵ_H cannot be assigned unequivocally to (−)-α-HCH dehydrochlorination (see discussion below and Section S4.3).

(+)-α-HCH Whereas (+)-α-HCH was not transformed in incubations at low enzyme concentrations (Figure 1D), it was completely turned over in incubations at high enzyme concentrations (0.7 μg mL^{-1}, Figure 1G). In such reactions, β-PCCH**1** appeared as transient species at concentrations

$\leq 3\mu$M, and 1,2,4-TCB became the final product. The C isotope signature of (+)-α-HCH in the course of the reaction is shown in Figure 1H and showed large isotope fractionation equivalent to an ϵ_C of -9.6 ± 0.1‰ (Table 1). In agreement with the fact that the final product of the dehydrochlorination of both β-PCCH enantiomers in incubations with LinA2 is 1,2,4-TCB, 1,2,4-TCB was the only accumulating final product. Figure 1H shows that late in the transformation reaction (i.e., after 25 min), the final δ^{13}C signature of 1,2,4-TCB became equal to the initial signature of α-HCH. Because (−)-α-HCH was transformed immediately in these reactors, we attributed the observable H isotope fractionation shown in Figure 1I to (+)-α-HCH with an enantiomer-specific ϵ_H, of -208 ± 19‰ for (+)-α-HCH (Table 1, Section S4.3).

LinB-catalyzed transformation reactions

Incubation of LinB with (−)-α-, β-, and δ-HCH resulted in their transformation by hydrolytic dechlorination. (+)-α-HCH was not transformed when incubated with LinB. As it was previously shown that γ-HCH is not a substrate of LinB,[26] we did not conduct experiments with γ-HCH. Catalytic efficiencies of LinB, k_{cat}/K_m, for the three substrates are given in Table 1.

δ-HCH

δ-HCH was completely transformed within 5 h when incubated with LinB (Figure 2A). Concomitantly, 2,3,4,5,6-pentachlorocyclohexane-1-ol (labelled D1[24] in Figure 2A) was transiently accumulating. Its disappearance after 2 h indicated the formation of the expected final product 2,3,5,6-tetrachlorocyclohexan-1,4-diol,[25] which we were not able to measure with our analytical setup. Figures 2B and C show the C and H isotope fractionation during hydrolytic dechlorination of δ-HCH. The C and H isotope enrichment factors, ϵ_C and ϵ_H, amounted to -11.4 ± 0.2‰ and -43 ± 24‰, respectively (Table 1).

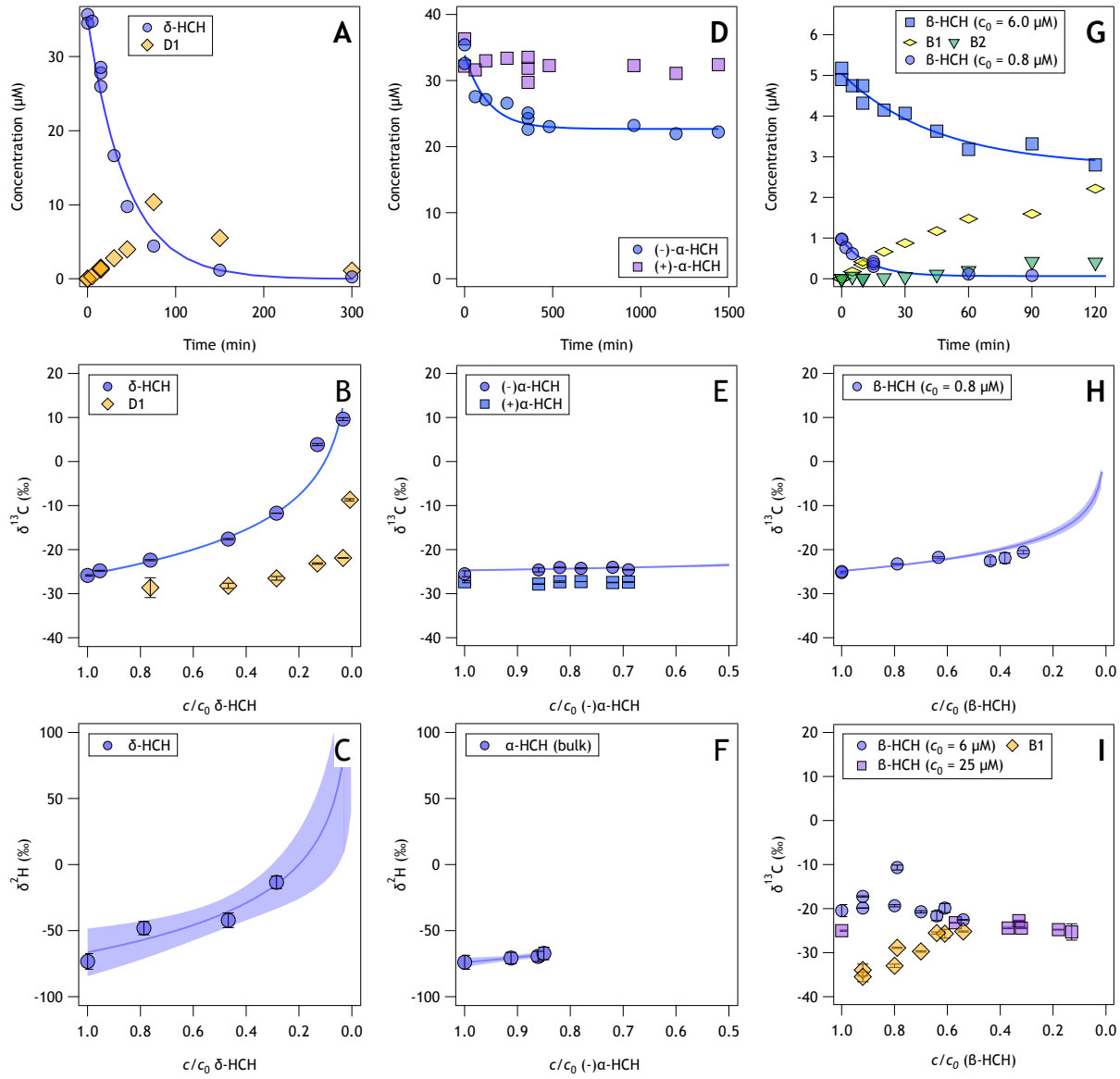

Figure 2 Concentration trends and C and H isotope fractionation associated with the hydrolytic dechlorination of δ-HCH (panels A-C), α-HCH (panels D-F), and β-HCH (panels G-H) in assays with LinB at pH 7.5. The top row, panels A, D and G, show measured and approximated concentrations of substrates and selected products. Solid lines represent best fits obtained for solving a series of ordinary differential equations.[34] The second row, panels B, E, H, and panel I in the third row show C isotope fractionation of substrates and selected products. Panels C and F illustrate substrate H isotope fractionation. Solid lines in panels B, C, E, F, and H are nonlinear fits to eq 3 and the shaded areas are 95% confidence intervals. Note that x-axes in panels E and F only show the first 50% of substrate disappearance, i.e., $c/c_0 > 0.5$ and that δ^{13}C values for $(+)$-α-HCH in panel E are plotted vs. c/c_0 of $(-)$-α-HCH.

(−)-α-HCH

Figure 2D shows that the (−)-α-HCH isomer was transformed only to a minor extent (30%) in a period of approximately 8 hours. The (+)-α-HCH enantiomer, however, was not transformed at all. The observable C fractionation of (−)-α-HCH was small (Figures 2E and F). ϵ_C amounted to -1.8 ± 0.8‰ (Table 1). The apparent H isotope fractionation again applies for the mixture of both α-HCH enantiomers (Figure 2F) and could be quantified with an ϵ_H of -39 ± 32‰. As illustrated in Section S4.3, this H isotope fractionation is most likely an artifact that could be the consequence of different initial δ^2H signatures, that is, isotopically heavy (−)-α- and light (+)-α-HCH. The exclusive reaction of (−)-α-HCH with more negative δ^2H by LinB would result in the accumulation of (+)-α-HCH and increase the δ^2H of the measured bulk α-HCH towards less negative values.

β-HCH

We observed the transformation of β-HCH by LinB at three different nominal initial concentrations (0.8, 6, and 25 μM). The results for experiments with the two smaller initial concentrations of β-HCH are shown in Figure 2G, the one for 25 μM in Figure S8A. The accumulation of the expected products, 2,3,4,5,6-pentachlorocyclohexan-1-ol (B1) and 2,3,5,6-tetrachlorocyclohexan-1,4-diol (B2),[25] is shown here for experiments with 6 μM β-HCH. Interestingly, we only observed C isotope fractionation in the experiments at lowest initial substrate concentrations (0.8 μM, Figure 2H) with an ϵ_C of -5.5 ± 0.8‰. Due to the low sensitivity of ^{2}H/^{1}H analysis, H isotope signatures of β-HCH could not be determined for this experiment. At higher initial concentrations of 6 and 25 μM, we were able to determine both C and H isotope signatures, but neither δ^{13}C nor δ^2H values of β-HCH changed during its transformation (Figures 2I and S8B, note that the used β-HCH specimen had different initial δ^{13}C values). In contrast, the δ^{13}C of 2,3,4,5,6-pentachlorocyclohexan-1-ol (B1), the first hydroxylated intermediate in the reaction, showed the typical trend for transient reaction product (Figure 2I). The difference of δ^{13}C between β-HCH and B1 amounted to -13.5 ± 1.5‰ and offers an alternative estimate for ϵ_C of β-HCH hydrolytic dechlorination (eq 4). Note that this ϵ_C is substantially larger than the value determined from C

isotope fractionation of the substrate β-HCH.

Discussion

Dehydrochlorination Catalyzed by LinA2

Enzyme Kinetics

All LinA2-catalyzed dehydrochlorinations of HCH led to PCCH intermediates that reacted further to different TCB isomers. The catalytic efficiency, k_{cat}/K_m, differed by four orders of magnitude from $8.9 \cdot 10^2$ to $5.6 \cdot 10^6$ $M^{-1}s^{-1}$ (Table 1). (−)-α-HCH was transformed most efficiently, followed by γ-HCH. LinA2 displayed similar k_{cat}/K_m-values for δ-HCH and (+)-α-HCH. We obtained a k_{cat}/K_m value for (−)-α-HCH transformation that was four orders of magnitude higher than that for (+)-α-HCH. In agreement with our data, Sharma et al.[44] reported turnover rates of purified LinA2 decreasing in the same sequence (α-HCH > γ-HCH > δ-HCH). While Sharma et al.[44] did not distinguish between α-HCH enantiomers, this preference of LinA2 for the (−)-α-HCH enantiomer over the (+)-α-HCH enantiomer has been reported before.[27,43] Despite the high k_{cat}/K_m-value, (−)-α-HCH was not completely turned over when incubated with LinA2 (Figure 1D, G). Residual (−)-α-HCH concentrations increased from 2.7 to 23 μM, corresponding to 7% and 45 respectively, of the initial substrate concentration, with decreasing enzyme concentrations (0.7 to 0.01 μg mL^{-1}). This observation suggests possible enzyme inhibition, as has been shown for LinA2 when incubated with racemic β-hexabromocyclododecane (β-HBCD).[45] There, Heeb et al.[45] showed that the (+)-β-HBCD enantiomer was turned over much faster when it was incubated with LinA2 as the pure (+)-enantiomer than when it was incubated with LinA2 as part of a racemic mixture.

Isotope Fractionation and Kinetic Isotope Effects

Despite substantial differences in catalytic efficiencies, carbon enrichment factors, ϵ_C, were similar for all HCH isomers (Table 1) and ranged from -8.3 ± 0.1 to -9.6 ± 0.1‰ for (+)-α-, γ-, and δ-HCH.

Table 1 Catalytic efficiencies, k_{cat}/K_m, C and H isotope enrichment factors, ϵ_C and ϵ_H, apparent ^{13}C- and ^{2}H kinetic isotope effects, ^{13}C- and ^{2}H-AKIE, and correlations of C vs. H isotope fractionation, $\Lambda^{H/C}$, for the dehydrochlorination and hydrolytic dechlorination of HCH isomers by LinA2 and LinB, respectively.[a]

	units	δ-HCH	γ-HCH [b]	β-HCH[c]	(+)-α-HCH	(−)-α-HCH
LinA2						
k_{cat}/K_m	($M^{-1}s^{-1}$)	$(9.0\pm0.1)\cdot10^{2}$	$(1.7\pm0.1)\cdot10^{4}$	n.d.[d,e]	$(8.9\pm0.1)\cdot10^{2}$	$(5.6\pm0.1)\cdot10^{6}$
ϵ_C	(‰)	−9.1±0.4	−8.3±0.1	n.d.	−9.6±0.1	−11.7±1.5 [f]
^{13}C-AKIE [g]	(-)	1.028±0.001	1.025±0.0005	n.d.	1.029±0.001	1.036±0.005
^{13}C-AKIE [h]	(-)	1.032±0.003	1.027±0.0005	n.d.	1.024±0.001	n.d.
ϵ_H	(‰)	−182±18	−160±6	n.d.	−208±19	n.a. [i]
^{2}H-AKIE [h]	(-)	4.2±0.1	2.6±0.1	n.d.	6.7±2.9	n.d.
$\Lambda^{H/C}$	(-)	19.2±1.5	16.4±0.9	n.d.	22.0±3.3	n.d.
LinB						
k_{cat}/K_m	($M^{-1}s^{-1}$)	$(1.2\pm0.1)\cdot10^{3}$	n.d.[j]	$(3.5\pm0.1)\cdot10^{4}$	n.d.	$(2.8\pm0.1)\cdot10^{2}$
ϵ_C	(‰)	−11.4±0.2	n.d.	−5.5±0.8	n.d.	−1.8±0.8
^{13}C-AKIE [g]	(-)	1.073±0.006	n.d.	1.034±0.005	n.d.	1.005±0.002
^{13}C-AKIE [h]	(-)	1.080±0.004	n.d.	n.d.	n.d.	n.d.
ϵ_H	(‰)	−43±24	n.d.	n.d.	n.d.	n.a. [i]
^{2}H-AKIE [h]	(-)	1.41±0.04	n.d.	n.d.	n.d.	n.d.
$\Lambda^{H/C}$	(-)	4.0±2.9	n.d.	n.d.	n.d.	n.d.

[a] Uncertainties denote 95% confidence intervals. [b] data from Schilling et al.[15] [c] data from experiments with LinB and initial β-HCH concentrations of 0.8 μM; [d] n.d. = not determined; [e] no transformation of β-HCH by LinA2;[8] [f] eq 4; [g] calculated according to eq 5; [h] from isotopomer model with eqs S7 and S8; [i] n.a. = not applicable, H isotope fractionation cannot be assigned to (−)-α-HCH enantiomer, see text and Section S4.3; [j] no transformation of γ-HCH by LinB.[26]

(−)-α-HCH showed no C isotope fractionation over the course of the reaction (see discussion below). Apparent ^{13}C-kinetic isotope effects, ^{13}C-AKIEs, derived from ϵ_C values, ranged from 1.025±0.005 to 1.029 ± 0.001 (Table 1) and were indicative of bimolecular elimination (E2) reactions when compared to both theoretical and experimental isotope effects of dehydrochlorination reactions. They were consistent with theoretical ^{13}C-KIEs computed by Saunders[46] for elimination reactions of ethyl chloride with different nucleophiles (1.015 to 1.032) as well as with the dehydrochlorination of polychlorinated ethanes (1.027 to 1.031).[47]

Hydrogen isotope enrichment factors, ϵ_H, describing the substantial H isotope fractionation observed in the substrates varied from −160 ± 6 to −208 ± 19‰ for (+)-α-, γ-, and δ-HCH. The ^{2}H-AKIEs calculated with an isotopomer-specific model (Section S4.2) spanned from 2.6 ± 0.1 to 6.7 ± 2.9 (Table 1) in agreement with the notion that cleavage of bonds to H contribute to the rate-limiting step of dehydrochlorination reactions (Scheme 2).[48–53] Variation of the large ^{2}H-AKIEs could be an indication that the timing of C–H and C–Cl bond breaking differs somewhat among HCH isomers despite transformation of all HCHs according to the same reaction mechanism. We assume that differences in the relative timing of proton transfer versus the cleavage of the C–Cl bond have caused the variations in H isotope fractionation.

Based on the same hypotheses, Manna and Dybala-Defratyka[54] computed ^{13}C- and ^{2}H-KIEs of HCH isomers reacting with LinA2 using density functional theory and continuum solvation models. Averaged predicted ^{13}C-KIEs were between 1.01 and 1.02 and thus substantially smaller than values measured here. For γ-HCH and δ-HCH transformation, ^{2}H-KIE-values between 4.1 to 5.1 and 3.0 to 5.1, respectively, were calculated. While the predictions for the ^{2}H-KIE of δ-HCH dehydrochlorination agree with our observations (4.2 ± 0.1), predictions for ^{2}H-AKIEs of γ-HCH were higher than we reported recently (2.6 ± 0.1).[15] Although the calculations of Manna and Dybala-Defratyka[54] revealed significant variations in ^{2}H-KIEs between HCH isomers, theory failed to correctly predict the variations among HCH isomers that we observed experimentally.

We observed substantial differences in isotope fractionation behavior between (+)-α-HCH and (−)-α-HCH (Figures 1E-F, H-I). While transformation of (+)-α-HCH was associated with the

strong C and H isotope fractionation considered indicative of dehydrochlorination by LinA2, data for (−)-α-HCH remain somewhat enigmatic. Despite absence of substrate isotope fractionation, the reaction product β-PCCH (Figure 1E) was depleted in ^{13}C to an extent that corresponds to an ϵ_C of -11.7 ± 1.5‰ and a ^{13}C-AKIE of 1.036 ± 0.005. These numbers are somewhat higher than for the other HCH isomers but still representative for isotope effects of E2 reactions. We hypothesize that the rate of (−)-α-HCH disappearance is not associated with bond cleavage but with another process such as the formation of the enzyme-substrate complex. It was shown for acetylcholinesterase, an enzyme whose rate-determining step is the diffusion-controlled encounter of the enzyme with free substrate,[55] that all the possible deuterium-substituted isomers of acetylcholine reacted at the same rate as acetylcholine itself.[56,57] There was no isotope effect associated with these reactions. The authors concluded that in this case, the rates of all chemical steps in the reaction sequence were more rapid than the encounter of the substrate with the active site of the enzyme.[57] In analogy, we interpret the absence of C isotope fractionation in the case of dehydrochlorination of (−)-α-HCH by LinA2 as indication that already a k_{cat}/K_m as high as $5.6 \cdot 10^6$ $M^{-1}s^{-1}$ identifies this reaction as diffusion-controlled. As noted above, while we observed no C isotope fractionation in (−)-α-HCH as a substrate, there was a significant enrichment of light C isotopes in the β-PCCH intermediate. In contrast to the concentrations-based mass balance with (−)-α-HCH and β-PCCH**2** in Figure 1D, the isotopic mass balance was not complete. This observation implies that some other species enriched in ^{13}C should exist in our system which we were unable to observe. To our knowledge, masking of substrate fractionation has never been observed in combination with visible isotope enrichment in the product. This phenomenon needs further investigation.

The observable H isotope fractionation at low LinA2 concentration shown in Figure 1F represents averaged data for both α-HCH enantiomers due to the lack of chromatographic resolution. We assigned this H isotope fractionation to the dehydrochlorination of (+)-α-HCH while δ^2H for the (−)-α-enantiomer should remain constant given that there was no C isotope fractionation for this compound. Even though (+)-α-HCH was transformed only to a minor extent (< 4%, Figure 1D), the substantial ^{2}H-AKIE of the (+)-α-enantiomer of 6.7 ± 2.9 is likely responsible for the observed

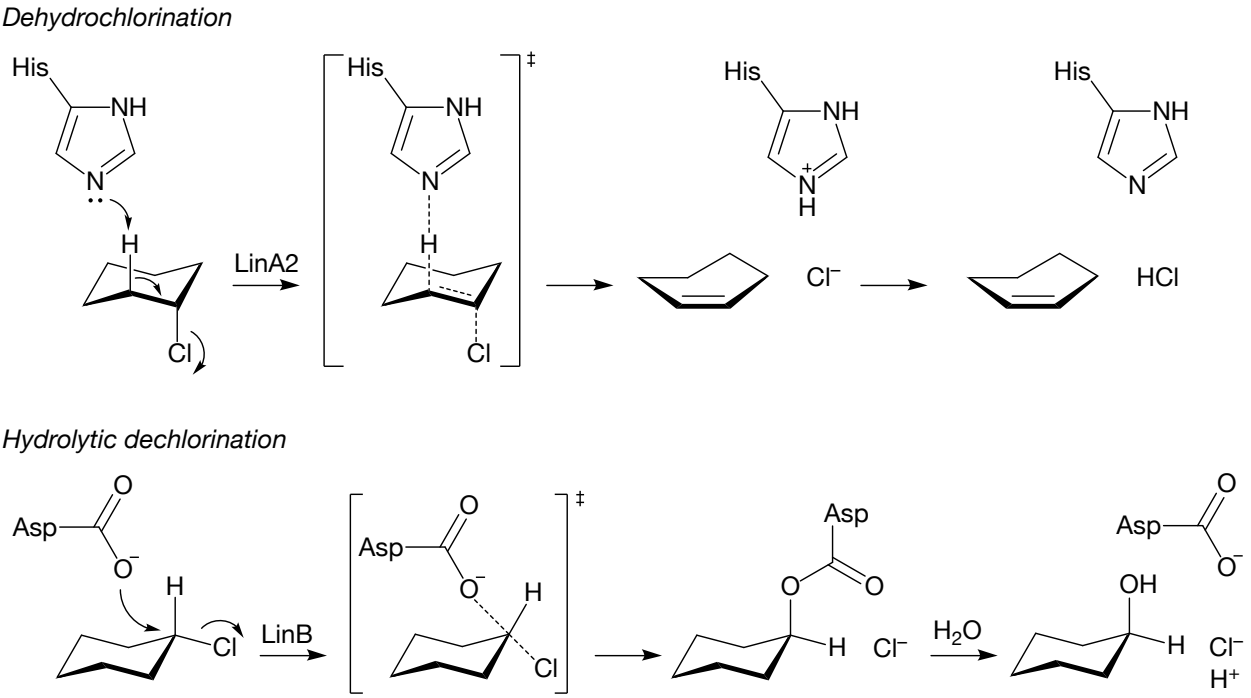

Scheme 2 Mechanisms and tentative transition state structures of HCH dehydrochlorination by LinA2 through bimolecular elimination (E2) and hydrolytic dechlorination by LinB through bimolecular nucleophilic substitution (S_N2) involving histidine and aspartate residues in the active site, respectively.[58,59] Note that Cl and H atoms in non-reactive positions are not drawn here for simplicity.

δ^2H trends in Figure 1F. Model calculations shown in Section S4.3 support this interpretation.

Bashir et al.[20] studied carbon isotope fractionation associated with the transformation of α-HCH in assays with whole cells of *S. indicum* B90A expressing LinA1, LinA2, and LinB. They reported isotope fractionation for both α-HCH enantiomers with ϵ_C-values of $-2.4 \pm 0.8‰$ and $-0.7 \pm 0.2‰$ for (+)-α-HCH and (−)-α-HCH, respectively. The apparent discrepancy between our data from pure enzyme assays and these of whole cell experiments performed by Bashir et al.[20] is likely due to the expression of both LinA1 and LinA2 variants in *S. indicum* B90A. As LinA1, which is known to transform (+)-α-HCH preferentially, also has some activity with (−)-α-HCH,[27] we suggest that the observed C fractionation of (−)-α-HCH in assays with whole cells was due to transformation by LinA1. More detailed data on the kinetic isotope effects of LinA1 and on isotopic masking in whole cell assays is necessary to confirm this interpretation.

Hydrolytic dechlorination catalyzed by LinB

Enzyme Kinetics

The catalytic efficiencies, k_{cat}/K_m, of LinB-catalyzed hydrolytic dechlorination of HCH isomers to pentachlorocyclohexanols ranged from $2.8 \cdot 10^2$ to $3.5 \cdot 10^4$ $M^{-1}s^{-1}$, with β-HCH being transformed the fastest followed by δ-HCH and (−)-α-HCH (Table 1). The k_{cat}/K_m-value of $9.4 \cdot 10^2$ $M^{-1}s^{-1}$ (Table S6) for the transformation of 6 μM of β-HCH by the LinB variant we studied here agreed well with those obtained with LinB variants originating from other bacteria ($1.9 \cdot 10^2$ to $1.0 \cdot 10^3$ $M^{-1}s^{-1}$).[60,61] We also obtained values that were one order of magnitude higher ($3.5 \cdot 10^4$ $M^{-1}s^{-1}$) at low substrate concentrations (0.8 μM) and ascribe this difference to the typical variability of biological replicates as well as uncertainties in the determination of enzyme concentrations. In assays with high initial concentration of β-HCH (25 μM), the substrate was not transformed completely (Figure S8A). This observation has also been reported previously for other variants of LinB.[24,61,62] Nagata et al.[61] showed that the best curve fit of the transformation of β-HCH catalyzed by LinB from *S. japonicum* UT26 was obtained when assuming product inhibition.

Although the transformation of δ-HCH by LinB has been studied previously,[24,25,63] no catalytic efficiencies or reaction constants have been published. Geueke et al.[24] reported that in incubations with the same amount of LinB as used here, δ-HCH was transformed completely after 24 hours, while 15-20% of the initial β-HCH still remained. In contrast to these findings, our experiments showed a 10-fold higher catalytic efficiency of LinB for transformation of β-HCH than for δ-HCH (Table 1). Based on the available data, we were unable to identify the reason for this discrepancy.

The transformation of α-HCH by LinB has been reported before,[24,26] but this study is the first to report enantiomer-specific transformation of α-HCH with LinB. We observed the selective yet incomplete degradation of (−)-α-HCH when incubated with 13-15 μg mL^{-1} LinB for 8 h. Geueke et al.[24] reported complete transformation of α-HCH after 24 hours of incubation with 16 μg mL^{-1} of the same LinB variant. Similar to observations for LinA2-catalyzed dehydrochlorination of α-HCH, we hypothesize that products or the non-reactive (+)-α-HCH inhibited LinB.

Isotope Fractionation and Kinetic Isotope Effects

We only obtained unambiguous C and H isotope enrichment factors for δ-HCH with an ϵ_C of -11.4 ± 0.2‰ and an ϵ_H of -43 ± 24‰ (Table 1). The C isotope enrichment for β- and (−)-α-HCH was substantially smaller with ϵ_C-values of -5.5 ± 0.8‰ and -1.8 ± 0.8‰, respectively. C isotope fractionation of β-HCH vanished as substrate concentrations increased from 0.8 to 25 μM. This trend suggests a masking of isotope fractionation through dissolution processes because of the limited aqueous solubility of of β-HCH.[6,64,65] The extent of (−)-α-HCH transformation, in contrast, was limited by the presence of the (+)-α-HCH enantiomer and/or reaction products. The quantification of C isotope fractionation in a substrate with such a low turnover is very uncertain.[50] The observed H isotope fractionation is likely an artifact of different initial δ^2H values of (−)-α- and (+)-α-HCH enantiomers. As is discussed in Section S4.3, the observed δ^2H trends could have been caused by the preferential reaction of isotopically heavy (−)-α-HCH and concomitant enrichment of the remaining enantiomer mixture with isotopically light (+)-α-HCH.

Due to these limitations, ^{13}C- and ^{2}H-AKIE-values for hydrolytic dechlorinations by LinB were derived from data for δ-HCH. The ^{13}C-AKIE of 1.073 ± 0.006 for the transformation of δ-HCH by LinB was distinctly higher than transformation of δ-HCH by LinA2 , whereas H isotope fractionation was smaller with a ^{2}H-AKIE of 1.41 ± 0.04 (Table 1). The high ^{13}C-AKIE of δ-HCH is in agreement with theoretical and experimental ^{13}C-AKIEs of bimolecular nucleophilic substitution (S_N2 type) reactions (Scheme 2) in which H atoms only experience secondary isotope effects while bonds to C are both broken and formed. ^{13}C-AKIEs range from 1.03 to 1.07 for halogenated hydrocarbons undergoing S_N2 type reactions.[66–69] ^{13}C-AKIEs of similar magnitude as found here for δ-HCH incubated with LinB were reported for the enzyme-catalyzed nucleophilic substitution of 1,2-dichlorethane in whole cell assays (1.068).[66] The ^{2}H-AKIE, on the other hand, was higher than observed typically for S_N2 and S_N1 type reactions.[67,68] Elsner et al.[67] inferred ^{2}H-KIEs from anaerobic S_N2 reactions[69] and reported values for methyl *tert*-butyl ether undergoing S_N2 reactions ranging from 1.05 to 1.09. Nevertheless, the moderately large ^{2}H-AKIE found here for the hydrolytic dechlorination of δ-HCH, illustrate that bond cleavage reactions determine the

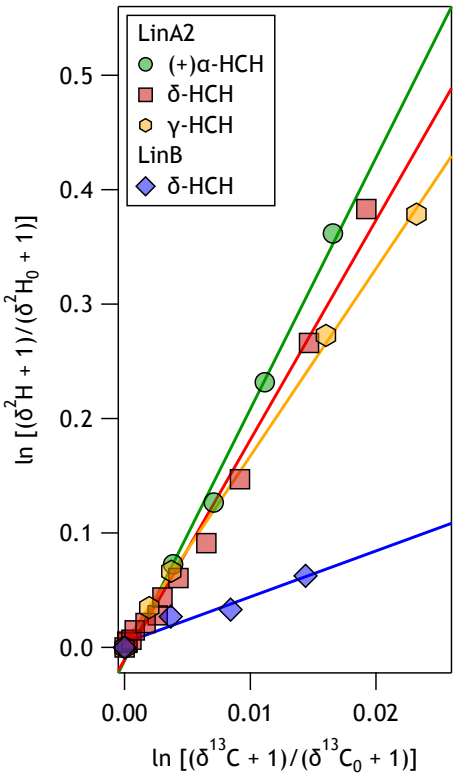

Figure 3 Correlation of C and H isotope fractionation associated with the dehydrochlorination of (+)-α-, γ-, and δ-HCH by LinA2 ($\Lambda^{H/C}$ = 16-22) and hydrolytic dechlorination of δ-HCH by LinB ($\Lambda^{H/C}$ = 4.0). The solid lines represent correlation slopes, $\Lambda^{H/C}$ (Table 1). Data for γ-HCH are reproduced from Schilling et al.[15]

rates of HCH transformation catalyzed by LinB.

Implications

Despite considerable substrate-dependency, we observed some general trends for the C and H isotope fractionation and isotope effects associated with the dehydrochlorination and hydrolytic dechlorination of HCH isomers by LinA2 and LinB, respectively. Figure 3 and the corresponding data in Table 1 illustrate that the two reactions differ primarily in the magnitude of H isotope fractionation whereas the magnitude of C isotope fractionation is about the same in both cases. As a consequence, the slopes of the correlation, $\Lambda^{H/C}$, are steeper for dehydrochlorination (i.e., between 16 and 22) than for hydrolytic dechlorination (4.0). These isotope fractionation patterns

are important benchmarks for the identification of the two initial biotransformation steps of HCHs under aerobic conditions.

While this study was carried out with purified enzymes and thus focussed on identifying isomer-specificities pertinent to the two reactions initiating aerobic HCH biodegradation and biotransformation, our work also offers insights for the application of CSIA at HCH-contaminated sites. First, even though data for isomer-specific isotope fractionation of HCH is scarce (Table S5) and restricted to C isotopes, the comparison of results from enzyme assays *vs.* whole cell systems for α- and γ-HCH[20] illustrates that the large ^{13}C-AKIEs are masked so that ϵ_C-values are up to 6-fold smaller when transformations occur in bacteria. This observation implies that future studies should also include the evaluation of additional isotopic elements such as H and Cl.[70–73] Assessing potentially small isotope fractionation of HCHs based on correlations of isotope fractionation such as $\Lambda^{H/C}$ shown in Figure 3 provides more reliable means to identify degradation processes in the environment. Second, our work also reveals that additional processes can bias the interpretation of isotope fractionation. The high catalytic efficiency of LinA2 with (−)-α-HCH and the ensuing diffusion limitation as well as the poor solubility of β-HCH both led to a situation, in which other processes than bond-cleavage reactions are determining the rate of HCH disappearance. In fact, dissolution processes of poorly soluble organic contaminants often play an essential role at contaminated sites. Finally, our comparison of isotope fractionation for HCH isomers that can be transformed with LinA and LinB points to possible complications through competitive, enzyme-catalyzed reactions. LinA and LinB are both critical for HCH-metabolism in HCH-degrading bacteria and the two enzymes are expressed constitutively in *Spingomondaceae*.[24,74] LinA catalyzes the first two dehydrochlorinations of γ-HCH and γ-PCCH on the pathway to mineralization, whereas LinB is involved in the transformation of tetra- and trichlorinated intermediates (Scheme 1). However, recent evidence suggests a competitive behavior of LinA and LinB towards transformation of HCH isomers.[24] It is thus conceivable that the biotransformation of the α-, β-, and δ-HCH isomers, which are not mineralized, could be caused by both dehydrochlorination by LinA and hydrolytic dechlorination by LinB. The observable C and H substrate isotope fractionation

would then represent a combination of the trends shown in Figure 3. In fact, it is unclear if such phenomena may have influenced the outcome of current studies in experiments with whole organisms. Further work exploring the modulation of contaminant isotope fractionation by the above mentioned factors is necessary to delineate conditions for a successful assessment of HCH degradation at contaminated sites by CSIA.

Acknowledgement

This work was supported by the SNSF (grant no. 200021-153534). We thank Thomas Fleischmann and Jakov Bolotin for analytical support.

Supporting Information Available

List of chemicals, solution, and isotopic standards used, protein expression and purification, experimental setup and chromatographic separations, data evaluation procedures, input parameters for isotopomer modeling, additional experimental data, molecular structures of substrates and products, and stereoisomers of PCCH. This material is available free of charge via the Internet at `http://pubs.acs.org/`.

References

(1) Vijgen, J. *The legacy of lindane HCH isomer production. A global overview of residue management, formulation and disposal*; International HCH & Pesticides Association (IHPA), http://www.ihpa.info/docs/library/reports/Lindane%20Main%20Report%20DEF20JAN06.pdf, 2006.

(2) Vijgen, J.; Abhilash, P.; Li, Y.; Lal, R.; Forter, M.; Torres, J.; Singh, N.; Yunus, M.; Tian, C.; Schaeffer, A.; Weber, R. Hexachlorocyclohexane (HCH) as new Stockholm Convention POPs - global perspective on the management of lindane and its waste isomers. *Environ. Sci. Pollut. Res.* **2011**, *18*, 152–162.

(3) Li, Y. Global technical hexachlorocyclohexane usage and its contamination consequences in the environment: from 1948 to 1997. *Sci. Total Environ.* **1999**, *232*, 121–158.

(4) Iwata, H.; Tanabe, S.; Sakai, N.; Tatsukawa, R. Distribution of persistent organochlorines in the oceanic air and surface seawater and the role of ocean on their global transport and fate. *Environ. Sci. Technol.* **1993**, *27*, 1080–1098.

(5) Buser, H.-R.; Mueller, M. D. Isomer and enantioselective degradation of hexachlorocyclohexane isomers in sewage sludge under anaerobic conditions. *Environ. Sci. Technol.* **1995**, *29*, 664–672.

(6) Slade, R. E. The gamma isomer of hexachlorocyclohexane (Gammexane). An insecticide with outstanding properties. *Chemistry & Industry* **1945**, 314–319.

(7) Geueke, B.; Miska, M. E.; Poiger, T.; Rentsch, D.; Lal, R.; Holliger, C.; Kohler, H.-P. E. Enantioselective dehydrochlorination of δ-hexachlorocyclohexane and δ-pentachlorocyclohexene by LinA1 and LinA2 from *Sphingobium indicum* B90A. *Appl. Environ. Microbiol.* **2013**, *79*, 6180–6183.

(8) Lal, R.; Pandey, G.; Sharma, P.; Kumari, K.; Malhotra, S.; Pandey, R.; Raina, V.; Kohler, H.-P. E.; Holliger, C.; Jackson, C.; Oakeshott, J. G. Biochemistry of microbial degradation of hexachlorocyclohexane and prospects for bioremediation. *Microbiol. Mol. Biol. R.* **2010**, *74*, 58–80.

(9) Vijgen, J.; Yi, L. F.; Forter, M.; Lal, R.; Weber, R. The legacy of lindane and technical HCH production. *Organohalog. Compd.* **2006**, *68*, 899–904.

(10) Vijgen, J.; de Borst, B.; Weber, R.; Stobiecki, T.; Forter, M. HCH and lindane contaminated sites: European and global need for a permanent solution for a long-time neglected issue. *Environ. Pollut.* **2019**, *248*, 696–705.

(11) Garg, N.; Lata, P.; Jit, S.; Sangwan, N.; Singh, A. K.; Dwivedi, V.; Niharika, N.; Kaur, J.; Saxena, A.; Dua, A.; Nayyar, N.; Kohli, P.; Geueke, B.; Kunz, P.; Rentsch, D.; Holliger, C.; Kohler, H.-P. E.; Lal, R. Laboratory and field scale bioremediation of hexachlorocyclohexane (HCH) contaminated soils by means of bioaugmentation and biostimulation. *Biodegradation* **2016**, *27*, 179–193.

(12) Dadhwal, M.; Singh, A.; Prakash, O.; Gupta, S.; Kumari, K.; Sharma, P.; Jit, S.; Verma, M.; Holliger, C.; Lal, R. Proposal of biostimulation for hexachlorocyclohexane (HCH)-decontamination and characterization of culturable bacterial community from high-dose point HCH-contaminated soils. *J. Appl. Microbiol.* **2009**, *106*, 381–392.

(13) Phillips, T. M.; Lee, H.; Trevors, J. T.; Seech, A. G. Full-scale in situ bioremediation of hexachlorocyclohexane-contaminated soil. *J. Chem. Technol. Biotechnol.* **2006**, *81*, 289–298.

(14) Raina, V.; Suar, M.; Singh, A.; Prakash, O.; Dadhwal, M.; Gupta, S. K.; Dogra, C.; Lawlor, K.; Lal, S.; van der Meer, J. R.; Holliger, C.; Lal, R. Enhanced biodegradation of hexachlorocyclohexane (HCH) in contaminated soils via inoculation with *Sphingobium indicum* B90A. *Biodegradation* **2008**, *19*, 27–40.

(15) Schilling, I. E.; Hess, R.; Rup, L.; Hofstetter, T. B.; Kohler, H.-P. E. Kinetic isotope effects of the enzymatic transformation of γ-hexachlorocyclohexane by the lindane dehydrochlorinase variants LinA1 and LinA2. *Environ. Sci. Technol.* **2019**, *53*, 2353–2363.

(16) Ivdra, N.; Herrero-Martin, S.; Fischer, A. Validation of user- and environmentally friendly extraction and clean-up methods for compound-specific stable carbon isotope analysis of organochlorine pesticides and their metabolites in soils. *J. Chromatogr. A* **2014**, *1355*, 36–45.

(17) Liu, Y.; Bashir, S.; Stollberg, R.; Trabitzsch, R.; Weil, H.; Paschke, H.; Nijenhuis, I.; Richnow, H.-H. Compound specific and enantioselective stable isotope analysis as tools to monitor transformation of hexachlorocyclohexane (HCH) in a complex aquifer system. *Environ. Sci. Technol.* **2017**, *51*, 8909–8916.

(18) Chartrand, M.; Passeport, E.; Rose, C.; Lacrampe-Couloume, G.; Bidleman, T. F.; Jantunen, L. M.; Sherwood Lollar, B. Compound specific isotope analysis of hexachlorocyclohexane isomers: a method for source fingerprinting and field investigation of in situ biodegradation. *Rapid Commun. Mass Spectrom.* **2015**, *29*, 505–514.

(19) Zhang, N.; Bashir, S.; Qin, J.; Schindelka, J.; Fischer, A.; Nijenhuis, I.; Herrmann, H.; Wick, L. Y.; Richnow, H. H. Compound-specific stable isotope analysis (CSIA) to characterize transformation mechanisms of α-hexachlorocyclohexane. *J. Hazard. Mater.* **2014**, *280*, 750–757.

(20) Bashir, S.; Fischer, A.; Nijenhuis, I.; Richnow, H.-H. Enantioselective carbon stable isotope fractionation of hexachlorocyclohexane during aerobic biodegradation by *Sphingobium* spp. *Environ. Sci. Technol.* **2013**, *47*, 11432–11439.

(21) Bashir, S.; Hitzfeld, K. L.; Gehre, M.; Richnow, H. H.; Fischer, A. Evaluating degradation of hexachlorcyclohexane (HCH) isomers within a contaminated aquifer using compound-specific stable carbon isotope analysis (CSIA). *Water Res.* **2015**, *71*, 187–196.

(22) Lian, S.; Nikolausz, M.; Nijenhuis, I.; Leite, A. F.; Richnow, H. H. Biotransformation and inhibition effects of hexachlorocyclohexanes during biogas production from contaminated biomass characterized by isotope fractionation concepts. *Bioresour. Technol.* **2018**, *250*, 683 – 690.

(23) Badea, S.-L.; Vogt, C.; Gehre, M.; Fischer, A.; Danet, A.-F.; Richnow, H.-H. Development of an enantiomer-specific stable carbon isotope analysis (ESIA) method for assessing the fate of α-hexachlorocyclohexane in the environment. *Rapid Commun. Mass Spectrom.* **2011**, *25*, 1363–1372.

(24) Geueke, B.; Garg, N.; Ghosh, S.; Fleischmann, T.; Holliger, C.; Lal, R.; Kohler, H.-P. E. Metabolomics of hexachlorocyclohexane (HCH) transformation: ratio of LinA to LinB determines metabolic fate of HCH isomers. *Environ. Microbiol.* **2013**, *15*, 1040–1049.

(25) Raina, V.; Hauser, A.; Buser, H. R.; Rentsch, D.; Sharma, P.; Lal, R.; Holliger, C.; Poiger, T.; Müller, M. D.; Kohler, H.-P. E. Hydroxylated metabolites of β- and δ-hexachlorocyclohexane: bacterial formation, stereochemical configuration, and occurrence in groundwater at a former production site. *Environ. Sci. Technol.* **2007**, *41*, 4292–4298.

(26) Raina, V.; Rentsch, D.; Geiger, T.; Sharma, P.; Buser, H. R.; Holliger, C.; Lal, R.; Kohler, H.-P. E. New metabolites in the degradation of α- and γ-hexachlorocyclohexane (HCH): pentachlorocyclohexenes are hydroxylated to cyclohexenols and cyclohexenediols by the haloalkane dehalogenase LinB from *Sphingobium indicum* B90A. *J. Agric. Food Chem.* **2008**, *56*, 6594–6603.

(27) Suar, M.; Hauser, A.; Poiger, T.; Buser, H.-R.; Müller, M. D.; Dogra, C.; Raina, V.; Holliger, C.; van der Meer, J. R.; Lal, R.; Kohler, H.-P. E. Enantioselective transformation of α-hexachlorocyclohexane by the dehydrochlorinases LinA1 and LinA2 from the soil bacterium *Sphingomonas paucimobilis* B90A. *Appl. Environ. Microbiol.* **2005**, *71*, 8514–8518.

(28) Bala, K.; Geueke, B.; Miska, M. E.; Rentsch, D.; Poiger, T.; Dadhwal, M.; Lal, R.; Holliger, C.; Kohler, H.-P. E. Enzymatic conversion of ϵ-hexachlorocyclohexane and a heptachlorocyclohexane isomer, two neglected components of technical hexachlorocyclohexane. *Environ. Sci. Technol.* **2012**, *46*, 4051–4058.

(29) Nagata, Y.; Endo, R.; Ito, M.; Ohtsubo, Y.; Tsuda, M. Aerobic degradation of lindane (γ-hexachlorocyclohexane) in bacteria and its biochemical and molecular basis. *Appl. Microbiol. Biotechnol.* **2007**, *76*, 741.

(30) Sharma, P.; Raina, V.; Kumari, R.; Malhotra, S.; Dogra, C.; Kumari, H.; Kohler, H.-P. E.; Buser, H.-R.; Holliger, C.; Lal, R. Haloalkane dehalogenase LinB is responsible for β- and δ-hexachlorocyclohexane transformation in *Sphingobium indicum* B90A. *Appl. Environ. Microbiol.* **2006**, *72*, 5720–5727.

(31) Pati, S. G.; Kohler, H.-P. E.; Hofstetter, T. B. Characterization of substrate, cosubstrate,

and product isotope effects associated with enzymatic oxygenations of organic compounds based on compound-specific isotope analysis. In *Measurement and Analysis of Kinetic Isotope Effects*; Harris, M. E., Anderson, V. E., Eds.; Methods in Enzymology; Academic Press, 2017; Vol. 596; pp 291–329.

(32) Kragten, J. Calculating standard deviations and confidence intervals with a universally applicable spreadsheet technique. *Analyst* **1994**, *119*, 2161–2165.

(33) Dunn, P. J. H.; Hai, L.; Malinovsky, D.; Goenaga-Infante, H. Simple spreadsheet templates for the determination of the measurement uncertainty of stable isotope ratio delta values. *Rapid Commun. Mass Spectrom.* **2015**, *29*, 2184–2186.

(34) Hoops, S.; Sahle, S.; Gauges, R.; Lee, C.; Pahle, J.; Simus, N.; Singhal, M.; Xu, L.; Mendes, P.; Kummer, U. COPASI - a complex pathway simulator. *Bioinformatics* **2006**, *22*, 3067–3074.

(35) Eichler, D. In *Physikochemische Eigenschaften, Verhalten und Analytik der HCH-Isomeren*; Deutsche Forschungsgemeinschaft (DFG),, Ed.; Hexachlorcyclohexan als Schadstoff in Lebensmitteln; Verlag Chemie, Weinheim, 1983; pp 65–72.

(36) Fiedler, H.; Hub, M.; Hutzinger, O. *Stoffbericht Hexachlorcyclohexan (HCH)*; Landesanstalt für Umweltschutz Baden-Württemberg, 1993.

(37) Artimo, P.; Jonnalagedda, M.; Arnold, K.; Baratin, D.; Csardi, G.; de Castro, E.; Duvaud, S.; Flegel, V.; Fortier, A.; Gasteiger, E.; Grosdidier, A.; Hernandez, C.; Ioannidis, V.; Kuznetsov, D.; Liechti, R.; Moretti, S.; Mostaguir, K.; Redaschi, N.; Rossier, G.; Xenarios, I.; Stockinger, H. ExPASy: SIB bioinformatics resource portal. *Nucleic Acids Res.* **2012**, *40*, W597–W603.

(38) Scott, K.; Lu, X.; Cavanaugh, C.; Liu, J. Optimal methods for estimating kinetic isotope effects from different forms of the Rayleigh distillation equation 1. *Geochim. Cosmochim. Acta* **2004**, *68*, 433–442.

(39) Elsner, M. Stable isotope fractionation to investigate natural transformation mechanisms of organic contaminants: principles, prospects and limitations. *J. Environ. Monit.* **2010**, *12*, 2005–2031.

(40) Wijker, R. S.; Adamczyk, P.; Bolotin, J.; Paneth, P.; Hofstetter, T. B. Isotopic analysis of oxidative pollutant degradation pathways exhibiting farge H Isotope fractionation. *Environ. Sci. Technol.* **2013**, *47*, 13459–13468.

(41) Reichert, P. AQUASIM – a tool for simulation and data analysis of aquatic systems. *Water Sci. Technol.* **1994**, *30*, 21–30.

(42) Dorer, C.; Höhener, P.; Hedwig, N.; Richnow, H.-H.; Vogt, C. Rayleigh-based concept to tackle strong hydrogen fractionation in dual isotope analysis - The example of ethylbenzene degradation by *Aromatoleum aromaticum*. *Environ. Sci. Technol.* **2014**, *48*, 5788–5797.

(43) Shrivastava, N.; Macwan, A. S.; Kohler, H.-P. E.; Kumar, A. Important amino acid residues of hexachlorocyclohexane dehydrochlorinases (LinA) for enantioselective transformation of hexachlorocyclohexane isomers. *Biodegradation* **2017**, *28*, 171–180.

(44) Sharma, P.; Pandey, R.; Kumari, K.; Pandey, G.; Jackson, C. J.; Russell, R. J.; Oakeshott, J. G.; Lal, R. Kinetic and sequence-structure-function analysis of known LinA variants with different hexachlorocyclohexane isomers. *PLoS ONE* **2011**, *6*, e25128.

(45) Heeb, N. V.; Wyss, S. A.; Geueke, B.; Fleischmann, T.; Kohler, H.-P. E.; Lienemann, P. LinA2, a HCH-converting bacterial enzyme that dehydrohalogenates HBCDs. *Chemosphere* **2014**, *107*, 194–202.

(46) Saunders, W. H. Heavy atom isotope effects in elimination reactions. An *ab initio* study. *Croat. Chem. Acta.* **2001**, *74*, 575–591.

(47) Hofstetter, T. B.; Reddy, C. M.; Heraty, L. J.; Berg, M.; Sturchio, N. C. Carbon and chlorine

isotope effects during abiotic reductive dechlorination of polychlorinated ethanes. *Environ. Sci. Technol.* **2007**, *41*, 4662–4668.

(48) Duarte, F.; Gronert, S.; Kamerlin, S. C. L. Concerted or stepwise: How much do free-energy landscapes tell us about the mechanisms of elimination reactions? *J. Org. Chem.* **2014**, *79*, 1280–1288.

(49) Fry, A. Isotope-effect studies of elimination reactions. *Chemical Society Reviews* **1972**, *1*, 163–210.

(50) Melander, L.; Saunders, W. H. *Reaction Rates of Isotopic Molecules*; 331 pp; John Wiley & Sons; Wiley Interscience Publication, 1980.

(51) Jia, Z. S.; Rudzinski, J.; Paneth, P.; Thibblin, A. Borderline between E1cB and E2 mechanisms. Chlorine isotope effects in base-promoted elimination reactions. *J. Org. Chem.* **2002**, *67*, 177–181, PMID: 11777456.

(52) Brown, K. C.; Romano, F. J.; Saunders Jr, W. H. Mechanisms of elimination-reactions. 34. Deuterium and nitrogen isotope effects and hammett correlations in the reaction of (2-arylethyl)trimethylammonium ions with hydroxide ion in mixtures of water and dimethylsulfoxide. *J. Org. Chem.* **1981**, *46*, 4242–4246.

(53) Saunders Jr, W. H.; Edison, D. H. Mechanisms of elimination reactions. IV. Deuterium isotope effects in E2 reactions of some 2-phenylethyl derivatives. *J. Am. Chem. Soc.* **1960**, *82*, 138–142.

(54) Manna, R. N.; Dybala-Defratyka, A. Insights into the elimination mechanisms employed for the degradation of different hexachlorocyclohexane isomers using kinetic isotope effects and docking studies. *J. Phys. Org. Chem.* **2013**, *26*, 797–804.

(55) Fersht, A. *Structure and mechanisms in protein science: A guide to enzyme catalysis and protein folding.*; W.H. Freeman and Company, 1998.

(56) Hogg, J. L.; Elrod, J. P.; Schowen, R. L. Transition-state properties and rate-limiting processes in the acetylation of acetylcholinesterase by natural and unnatural substrates. *J. Am. Chem. Soc.* **1980**, *102*, 2082–2086.

(57) Schowen, K. B.; Schowen, R. L. The use of isotope effects to elucidate enzyme mechanisms. *BioScience* **1981**, 826–831.

(58) Manna, R. N.; Zinovjev, K.; Tunon, I.; Dybala-Defratyka, A. Dehydrochlorination of hexachlorocyclohexanes catalyzed by the LinA dehydrohalogenase. A QM/MM study. *J. Phys. Chem. B* **2015**, *119*, 15100–15109.

(59) Prokop, Z.; Monincova, M.; Chaloupkova, R.; Klvana, M.; Nagata, Y.; Janssen, D. B.; Damborsky, J. Catalytic mechanism of the haloalkane dehalogenase LinB from *Sphingomonas paucimobilis* UT26. *J. Biol. Chem.* **2003**, *278*, 45094–45100.

(60) Okai, M.; Ohtsuka, J.; Imai, L. F.; Mase, T.; Moriuchi, R.; Tsuda, M.; Nagata, K.; Nagata, Y.; Tanokura, M. Crystal structure and site-directed mutagenesis analyses of haloalkane dehalogenase LinB from *Sphingobium* sp. strain MI1205. *J. Bacteriol.* **2013**, *195*, 2642–2651.

(61) Nagata, Y.; Prokop, Z.; Sato, Y.; Jerabek, P.; Kumar, A.; Ohtsubo, Y.; Tsuda, M.; Damborskỳ, J. Degradation of β-hexachlorocyclohexane by haloalkane dehalogenase LinB from *Sphingomonas paucimobilis* UT26. *Appl. Environ. Microbiol.* **2005**, *71*, 2183–2185.

(62) Ito, M.; Prokop, Z.; Klvana, M.; Otsubo, Y.; Tsuda, M.; Damborsky, J.; Nagata, Y. Degradation of β-hexachlorocyclohexane by haloalkane dehalogenase LinB from γ-hexachlorocyclohexane-utilizing bacterium Sphingobium sp. MI1205. *Arch. Microbiol.* **2007**, *188*, 313–325.

(63) Wu, J.; Hong, Q.; Sun, Y.; Hong, Y.; Yan, Q.; Li, S. Analysis of the role of LinA and LinB in biodegradation of δ-hexachlorocyclohexane. *Environ. Microbiol.* **2007**, *9*, 2331–2340.

(64) Callahan, M. A.; Slimak, M.; Gabel, N.; May, I.; Fowler, C.; Freed, J.; Jennings, P.; Durfee, R.; Whitmore, F.; Maestri, B.; Maybe, W.; Holt, B.; Bould, C. *Water-related environmental fate of 129 priority pollutants*; U.S. Environmental Protection Agency Volume I: Introduction and technical background metals and inorganics pesticides and PCBs, 1979.

(65) NTP (National Toxicology Program), *Lindane, hexachlorocyclohexane (technical grade), and other hexachlorocyclohexane isomers*; U.S. Department of Health and Human Services, Public Health Service Report on Carcinogens, 14^{th} edition (https://ntp.niehs.nih.gov/go/roc14/), 2016.

(66) Palau, J.; Marchesi, M.; Chambon, J. C.; Aravena, R.; Canals, A.; Binning, P. J.; Bjerg, P. L.; Otero, N.; Soler, A. Multi-isotope (carbon and chlorine) analysis for fingerprinting and site characterization at a fractured bedrock aquifer contaminated by chlorinated ethenes. *Sci. Total Environ.* **2014**, *475*, 61–70.

(67) Elsner, M.; Zwank, L.; Hunkeler, D.; Schwarzenbach, R. P. A new concept linking observable stable isotope fractionation to transformation pathways of organic pollutants. *Environ. Sci. Technol.* **2005**, *39*, 6896–6916.

(68) Matsson, O.; Dybala-Defratyka, A.; Rostkowski, M.; Paneth, P.; Westaway, K. C. A theoretical investigation of α-carbon kinetic isotope effects and their relationship to the transition-state structure of SN2 reactions. *J. Org. Chem.* **2005**, *70*, 4022–4027.

(69) Kuder, T.; Wilson, J. T.; Kaiser, P.; Kolhatkar, R.; Philp, P.; Allen, J. Enrichment of stable carbon and hydrogen isotopes during anaerobic biodegradation of MTBE: Microcosm and field evidence. *Environ. Sci. Technol.* **2005**, *39*, 213–220.

(70) Renpenning, J.; Kummel, S.; Hitzfeld, K. L.; Schimmelmann, A.; Gehre, M. Compound-specific hydrogen isotope analysis of heteroatom-bearing compounds via gas chromatography–chromium-based high-temperature conversion (Cr/HTC)–isotope ratio mass spectrometry. *Anal. Chem.* **2015**, *87*, 9443–9450.

(71) Renpenning, J.; Hitzfeld, K. L.; Gilevska, T.; Nijenhuis, I.; Gehre, M.; Richnow, H.-H. Development and validation of an universal interface for compound-specific stable isotope analysis of chlorine (37Cl/35Cl) by GC-high-temperature conversion (HTC)-MS/IRMS. *Anal. Chem.* **2015**, *87*, 2832–2839, PMID: 25647449.

(72) Renpenning, J.; Schimmelmann, A.; Gehre, M. Compound-specific hydrogen isotope analysis of fluorine-, chlorine-, bromine-and iodine-bearing organics using gas chromatography–chromium-based high-temperature conversion (Cr/HTC) isotope ratio mass spectrometry. *Rapid Commun. Mass Spectrom.* **2017**, *31*, 1095–1102.

(73) Renpenning, J.; Horst, A.; Schmidt, M.; Gehre, M. Online isotope analysis of 37Cl/35Cl universally applied for semi-volatile organic compounds using GC-MC-ICPMS. *J. Anal. At. Spectrom.* **2018**, *33*, 314–321.

(74) Suar, M.; Van Der Meer, J. R.; Lawlor, K.; Holliger, C.; Lal, R. Dynamics of multiple *lin* gene expression in *Sphingomonas paucimobilis* B90A in response to different hexachlorocyclohexane isomers. *Appl. Environ. Microbiol.* **2004**, *70*, 6650–6656.

Graphical TOC Entry